Thermally stimulated power law relaxation of radiation-induced defects in K-feldspar

2007 J. Phys.: Condens. Matter 19 046202

(http://iopscience.iop.org/0953-8984/19/4/046202)

INSTITUTE OF PHYSICS PUBLISHING JOURNAL OF PHYSICS: CONDENSED MATTER

J. Phys.: Condens. Matter **19** (2007) 046202 (11pp) doi:10.1088/0953-8984/19/4/046202

Thermally stimulated power law relaxation of radiation-induced defects in K-feldspar

L Sánchez-Muñoz[1,3], J García-Guinea[2], V Correcher[1] and A Delgado[1]

[1] CIEMAT, Avenida Complutense 22, 28040 Madrid, Spain
[2] MNCN-CSIC, c/ José Gutierrez Abascal 2, 28006 Madrid, Spain

E-mail: luis.sanchez@ciemat.es

Received 3 October 2006, in final form 4 December 2006
Published 12 January 2007
Online at stacks.iop.org/JPhysCM/19/046202

Abstract

Thermally stimulated relaxation of x-ray irradiation-induced defects in a K-feldspar crystal, $Or_{93\pm2}Ab_{7\pm2}$, from Minas Gerais (Brazil), has been studied from the blue light emission obtained with a high sensitivity thermoluminescence spectrometer. Diffractometric analysis shows a small but observable departure from the monoclinic symmetry. A modulated structure is observed using transmission electron microscopy. The relaxation dynamics was monitored with a glow curve at 440 nm with maximum at 130 °C. It shows Arrhenius behaviour in the low temperature slope (activation energy 0.92 ± 0.02 eV) because relaxation is thermally activated by dispersive ionic diffusion. In the high temperature slope a power law close to exponential behaviour is found. The slight non-exponentiality is linked with the small triclinic distortion of the lattice and thus with elastic strain fields from the modular nature of the lattice. A feedback relationship between local defect relaxation and global modifications of the elastic strain field could give rise to an avalanche effect that would explain the power law statistics.

1. Introduction

Non-equilibrium states are induced in crystals when they are irradiated with ionizing radiation. During irradiation, crystals can be considered as open systems capable of structural pattern formation by global self-organization due to local reordering from cooperative atomic rearrangements (Ghoniem *et al* 2002). Metastable states are finally induced in the lattices because of the ionizations and the radiolytic defects. Thus, crystals have the capability of the storage of energy by electron–hole trapping processes, for example in luminescent defect complexes. Lattices recover to more stable states by relaxation on a wide range of timescales. The evolution of disequilibrated systems towards equilibrium follows exponential behaviour in

[3] Author to whom any correspondence should be addressed.

simple systems in which the relaxing units behave randomly, individually and independently. The non-exponential relaxation, following stretched exponentials or power law decays, emerges in complex systems by local cooperation during the rearrangement of the elementary units (Böhmer *et al* 1993) and/or strongly collective behaviour of such molecular entities (Jonscher *et al* 2003). When considering luminescent defects, four mechanisms have been proposed to explain the departure from exponential behaviour during their relaxation, namely: (i) retrapping (Chen and Leung 2003); (ii) tunnelling (Huntley 2006); (iii) dispersive diffusion in disordered systems (Pavesi and Ceschini 1993); and (iv) many-body interactions dominating the dynamics of charge release from trapping centres (Jonscher and de Polignac 1984).

A possible material to check these ideas against is K-feldspar ($K \gg Na)AlSi_3O_8$ since the relaxation decay of the luminescent defects does not follow an exponential behaviour. Specifically, the phosphorescence dynamics, the decay of optically excited luminescence, and the reduction in natural infrared stimulated luminescence and thermoluminescence (TL), as well as induced bleaching on exposure to sunlight, are known to follow power law decays (Huntley 2006, Baril and Huntley 2003, Bailiff and Barnett 1994, Wintle 1997, Duller 1997). A power law has also been found in the high temperature slope of the TL spectra of some emission bands (Sánchez-Muñoz *et al* 2006b). This mineral can be used in dose reconstruction and dating (Bøtter-Jensen *et al* 2003) applications because it exhibits the features required for a dosimeter, i.e. high sensitivity to ionizing radiation, reproducibility, and good dose linearity in the ranges of interest. The mineral structure is formed by a three-dimensional tetrahedral network of AlO_4 and SiO_4 units with alkali ions for the local electrostatic compensation occupying irregular sites. It shows mainly three structural states: (i) the high temperature monoclinic $C2/m$ phase is termed *sanidine*; (ii) *high microcline* (or orthoclase) is a 'transitional structure' exhibiting a metastable mesoscopic modulated structure; (iii) the low temperature triclinic $C\bar{1}$ phase is called *low microcline*, whose structure in most cases appears with regular twinning (Smith and Brown 1988).

In particular, microcline is the best candidate to use to check the aforementioned hypothesis since microcline crystals have shown the capability of self-organization. This adaptive behaviour during the high-to-low transformation has been induced by observations at the macroscopic scale. It occurred under tectonic shear stress stimulation with some water molecules as catalyst, as well as under the effect of ionizing radiation that induced radiolytic defects preferentially at coherent wall boundaries (Sánchez-Muñoz *et al* 2006a, 2006c). In addition, the exsolved Na-feldspar discrete domains at high temperature dispersed into the K-feldspar matrix of certain perthitic textures can coalesce to form clusters with self-similar shape and scale-free size distribution (Sánchez-Muñoz 1992). From these results, it is possible to speculate that self-organization could also operate at the local scale when K-feldspars are irradiated, for instance during the relaxation of the radiation-induced defects.

Ionizing radiation induces metastable hole centres in the oxygen sites of the structural framework of K-feldspars (O^- centres), as well as electrons trapped in oxygen vacancies (E centres), Petrov (1994) and Matyash *et al* (1982). The first defect is well known to be related to a broad blue emission band in a range 350–550 nm, with the maximum at about 440 nm, particularly on the Al–O–Al bridges (Speit and Lehmann 1982), that can be recorded for example using TL. However, some practical limitations exist in studying these defects, depending on the nature of the experimental material and methodology. Unaltered crystals must be studied because drastic modifications occur during interaction with water at low temperatures that decrease substantially the lattice sensitivity to ionizing radiation, i.e. water acts as a luminescence quencher (Hashimoto *et al* 2003). Furthermore, precise analyses of this band in K-feldspar cannot be performed using standard two-dimensional (2D)-plot TL methodologies (temperature versus intensity plots) when filters are disposed to collect

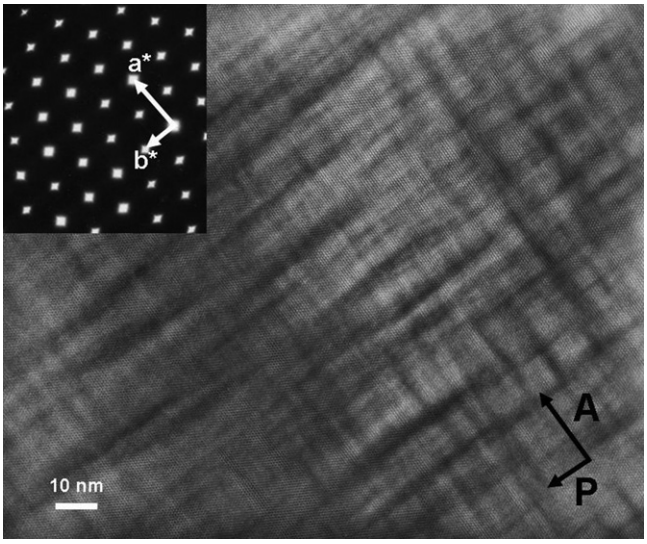

Figure 1. Low magnification high resolution image along the [001] zone axis showing the 'tweed' contrast by orthogonal wavelike bright–dark alternation obtained by electron transmission microscopy, with *A* along the (010) boundaries (composition plane of albite twin-law) and with *P* along the '*b*-axis' (twin axis of pericline twin-law). It includes the electron diffraction pattern (inset) of the same area in which a^* and b^* axis are marked. Note the orthogonal streaking of the diffraction spots.

the maximum intensity of light, i.e. the 7-59 + BG 39 configuration, since the broad blue luminescence emission can be overlapped by the 290, 340 and 400 nm emission bands (Prescott and Fox 1993, Correcher and Garcia-Guinea 2001). Thus, high resolution of 3D-plot TL with temperature–intensity–wavelength spectra is indispensable.

The aim of this article is to analyse the thermally stimulated relaxation of the non-equilibrium state induced in K-feldspar by x-ray irradiation. In particular, the relaxation of radiation-induced defects has been studied by the characteristics of the blue luminescence in a crystal with pristine features from high resolution TL spectra.

2. Experimental procedure

Material

The sample used in this work (F4 specimen) is an irregular giant crystal of perthitic K-feldspar about $0.5 \times 0.5 \times 0.25$ m^3 in size, from the intermediate zone of a granite pegmatite in Lavra Fermin in Linopolis, Minas Gerais (Brazil). Under the optical microscope, it shows irregular extinction at an angle of about 8° in (001), and albite–pericline twinning cannot be detected. The crystal exhibits extended pristine areas, as the preservation of the modulated structure guarantees (see figure 1), although some coarsened Na-feldspar perthitic veins also appear. The observation of the cathodoluminescence light emission under optical microscopy in thin section displays intense blue luminescence in the K-feldspar only, this being imperceptible in Na-feldspar. In consequence, the presence of Na-feldspar veins must not significantly interfere with the blue thermoluminescence signal from the K-feldspar.

Table 1. Bulk chemical composition of the specimen from XRF analyses in oxides of major elements and loss ignition (LI) in wt%; trace elements are in ppm.

SiO_2	Al_2O_3	P_2O_5	TiO_2	MgO	K_2O	Na_2O	CaO	MnO	LI	
64.70	18.95	0.78	<0.01	<0.01	12.21	2.77	<0.01	<0.01	0.53	
Cs	Rb	Ba	Sr	La	Ce	Y	Cu	Co	Ni	Cr
17	605	101	1	1	3	8	7	2	4	10

Chemical composition

Bulk chemical analyses of major and trace elements (table 1) of a powdered aliquot from the crystal were performed by spectrometry of x-ray fluorescence (XRF) using a Philips PW-1404, in Museo Nacional de Ciencias Naturales (MNCN) de Madrid (Spain). Chemical composition was performed by electron probe microanalysis (EPMA) using an SX-50 with the ZAF program to correct the matrix effects, at 15 kV, 25 nA and 1 μm spot diameter as operating conditions, in Centre de Recherches sur la Synthése et la Chimie des Mineraux (CRSCM, CNRS, Orléans (France).

X-ray diffraction

The crystal was studied by powder x-ray diffraction (XRD) using a Siemens D-5000 automated diffractometer with Cu Kα_1 radiation at 40 kV and 30 nA with Si as internal standard, scanning from 2° to 64° 2θ in steps of 0.020°, and with a counting time of 6 s per step, in MNCN. The Δ and Σt_1 parameters are supposed to report on the unit cell triclinicity and the Si/Al order in tetrahedral sites, and they were respectively calculated from the splitting of (131) and $(1\bar{3}1)$ diffractions and the positions of the (060) and $(\bar{2}04)$ peaks, (Kroll and Ribbe 1987).

Electron microscopy

Transmission electron microscopy (TEM) micrographs and selected area electron diffraction (SAED) patterns along the [001] zone axis (a^*b^* plane) were obtained in a JEOL 4000 EX instrument operating at 400 kV, using a thin foil sample prepared by ionic thinning (Ar at 15°) to obtain a preparation with transparency enough to electrons in a Gatan Duo Mill 600, in EMAT, Antwerpen (Belgium).

Thermoluminescence spectra

Spectra were obtained from cleaved chips of $3 \times 3 \times 2$ mm^3 ($\sim$5 mg) of this specimen mounted with silicone oil onto an aluminium disc using the TL spectrometer of Sussex University (United Kingdom). Signals were recorded over the 200–800 nm wavelength range, with a resolution of 4 nm for 150 point spectra, in the range 20–400 °C at 2.5 °C s^{-1}. All signals were corrected for the spectral response of the system. X-ray induced defects were studied by TL, after 50 Gy X-irradiation with an x-ray unit tube, Philips MG MCN 101, with a current of 5 mA and a voltage of 5 kV delivering a dose rate of 10 Gy min^{-1} to the sample. Prior to measurements, the sample was stored for 24 h under red light. Sample processing and measurements were also performed under red light to avoid electron–hole recombination from the metastable sites.

3. Results

Table 1 shows the bulk chemical composition from XRF analysis. Very low contents in Fe, Mg, Ti and Ca indicate the absence of dark mineral and plagioclase crystals as inclusions of impurities. The low lost ignition value indicates that the alteration to kaolinite is negligible. The Na_2O content is consistent with the observed perthitic intergrowth formed by a K-feldspar matrix and Na-feldspar discrete domains at ∼15 wt%, as observed by optical microscopy. The high contents in Rb, Cs and Ba are typical of samples with a limited evolution by recrystallization during the subsolidus and hydrothermal stages as these elements are lixiviated if water-rich fluid interactions with the crystal occur at low temperature. The contents of the other trace elements also indicate the absence of substantial alteration and impurities. The composition of the K-feldspar by EPMA is $Or_{93\pm2}Ab_{7\pm2}$, as a molar expression for the proportion of K- and Na-feldspar in the solid solution.

The XRD powder pattern of the K-feldspar shows peaks from the high microcline structure type only. The hypothetical unit cell triclinicity taken from the Δ parameter is 0.00, as (131) and $(1\bar{3}1)$ splitting is not observed. The Σt_1 parameter is 0.87 ± 0.01, higher than the value of 0.69 that indicates the separation of monoclinic and triclinic K-feldspar lattices (Bambauer *et al* 1989). Figure 1 shows the micrograph obtained by electron microscopy with the typical 'tweed' contrast characteristic of this structural state with alternating dark and white irregular lens-shaped bands, perhaps related to elastic strain fields from local transformation nano-avalanches, in which sharp boundaries between them cannot be observed. Note the self-similar morphological character and the scale-free size distribution of regions with dark and white contrasts, exhibiting the fractal nature of this modulated structure. The SAED pattern along the [001] zone axis (figure 1) indicates modulations along ($hk0$) planes by diffuse streaks parallel to the a^* and b^* axes. This could suggest a continuous and modulated departure from monoclinic symmetry along the crystal. A careful measurement of the γ^* angle indicates that a small deviation from 90° exists, as has been detected in similar feldspars. Thus, the x-ray powder pattern cannot detect the triclinic deviation because the small local continuous deviation from monoclinic symmetry. Actually, the domain size for coherent x-ray diffraction is higher than the size of the observed nanodomains (Ribbe 1983, Sánchez-Muñoz *et al* 1998).

Natural TL (NTL) and x-ray induced TL (ITL) high resolution spectra of the K-feldspar are represented using 3D-plots displaying intensity I (in arbitrary units, au) versus temperature T (in °C) and wavelength λ (in nm) in figures 2(a) and (c) and contour plots in the wavelength–temperature plane in figures 2(b) and (d). Four different light emissions are detected in the NTL spectrum at a temperature higher than 200 °C: (i) an intense and sharp Gaussian signal at ∼290 nm, showing a maximum intensity at around 350 °C typical of both triclinic K-feldspars and triclinic Na-feldspars; (ii) a weak emission at 340 nm characteristic of K-feldspars; (iii) an irregular signal centred at 400 nm typically used in most of the TL applications of K-feldspars; and (iv) a very weak emission at 570 nm due to radiative recombination in Mn^{2+} centres from the Na-feldspar vein intergrowths, as observed by cathodoluminescence images at the resolution of the optical microscope. The ITL spectrum was recorded after 50 Gy x-ray irradiation and differs significantly from the NTL spectrum in shape and intensity. It shows mainly two intense light emissions: (i) a sharp and intense ultraviolet signal appearing at ∼290 nm, being similar to that of the NTL but with a very irregular shape on the temperature axis, from 80 °C up to >400 °C and with maximum intensity circa 225 °C, from both phases; and (ii) a broad blue band centred at 440 nm, i.e. the broad blue luminescence signal from radiation-induced defects (O^- centres) (Speit and Lehmann 1982, Hashimoto *et al* 2003) with maximum intensity appearing at 130 °C that separates two different slopes along the temperature axis.

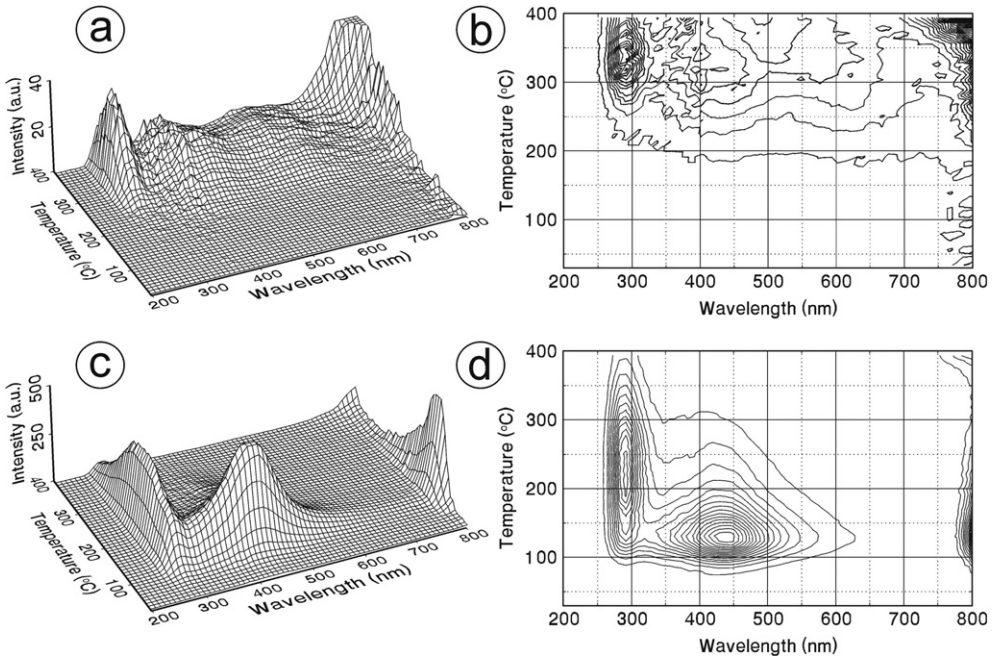

Figure 2. (a) and (b) Natural TL spectra, in a isometric plot and contour plot respectively, displaying intensity in arbitrary units, versus temperature T in °C, and wavelength λ in nm, (c) and (d) x-ray induced TL after 50 Gy irradiation in similar plots. The heating rate was 2.5 °C s^{-1}.

The glow peak at a fixed 440 nm wavelength, i.e. the monochromatic 2D spectrum of intensity versus temperature (figure 3(a)), is asymmetric. Simple numerical analysis fail to identify the well-known profiles of first- or second-order kinetics recognized in classical TL dosimetry materials because of the high temperature slope of the glow peak. However, the two slopes of the signal can be analysed with simple numerical expressions, signifying distinct phenomena occurring separately but being intrinsically correlated.

From the low temperature slope it is possible to calculate the activation energy (E_a in eV) by a thermally activated process. The initial rise method, from room temperature to 115 °C (figure 3(b)), was used. It assumes a constant number of electrons trapped in the low temperature tail of the analysed peak. Thus, the initial part of the TL glow peak might follow an exponential dependence regardless of the kinetic order and the assumption of the quasi-equilibrium approximation that is necessary to solve the equation (1):

$$I_{TL} \sim \exp(-E_a/kT) \tag{1}$$

where I_{TL} is the intensity of the TL emission (in arbitrary units, au), k is the Boltzmann's constant and T is the absolute temperature (in Kelvin, K). The Arrhenius plot ($\ln I_{TL}$ versus $1/T$) allows us to calculate the activation energy E_a from the slope $-E/k$ that is not dependent on the order of the kinetics (Furetta 2003). The estimated E_a in the range 76–113 °C with this method was 0.92 ± 0.02 eV.

The high temperature slope can be reproduced reasonably with a second-order exponential function (figure 3(c)) $r = 0.988$, (2):

$$I = A\exp(-T/t_1) + B\exp(-T/t_2) + y_0 \tag{2}$$

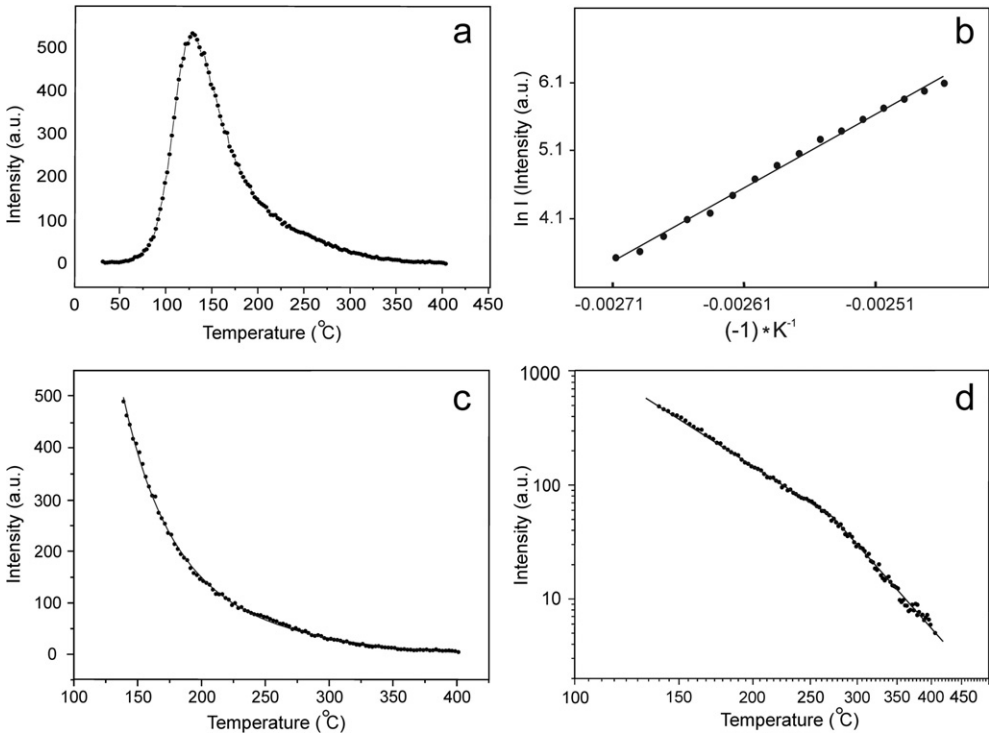

Figure 3. (a) TL slice at 440 nm from spectrum of figure 1(c) between RT and 400 °C. (b) Low-T side of the TL curve with an exponential analysis using the initial rise method (IRM) with an Arrhenius plot of $\ln I = \ln s - E_a/kT$ (where s is the pre-exponential factor, and E_a is the thermal activation energy) with $E_a = 0.92 \pm 0.02$ eV. (c) High-T side of the TL curve with a second-order exponential fitting using the expression $I = A\exp(-T/t_1) + B\exp(-T/t_2) + y_0$ (see table 2). (d) The same, with a logarithmic analysis by a two-segment power law using a $\log I = C - \tau \log T$ plot where τ are the coefficients (see table 3).

Table 2. Parameters from exponential fitting of the high temperature slope of the 440 nm emission band ($r = 0.988$).

Parameters	Values
y_0	-9.23 ± 5.03
A	$22\,050 \pm 6857$
t_1	31.57 ± 3.80
B	1121 ± 595
t_2	89 ± 16.8

where t_1 and t_2 are the coefficients for the low and high temperature parts (see parameters in table 2), but a very precise fitting was obtained using power laws in two segments, as illustrated in the log–log plot (figure 3(d)). In this case the lineal correlation factors are $r_1 = 0.999$ and $r_2 = 0.990$, when using the expression (3):

$$\log I = C - \tau \log T \tag{3}$$

where τ is the scaling coefficient (see the parameters in table 3).

Table 3. Parameters from the two-segment power law fittings of the high temperature slope of the 440 nm emission band ($r = 0.999$ for $T < 270\,^{\circ}$C, $r = 0.990$ for $T > 270\,^{\circ}$C).

Parameters	$T < 270\,^{\circ}$C value $\pm$ uncer.	$T > 270\,^{\circ}$C value $\pm$ uncer.
C	9.9 ± 0.04	15.8 ± 0.29
τ	3.4 ± 0.02	5.8 ± 0.12

4. Discussion

Exponential versus power law

The slopes of some TL glow curves in K-feldspars seem to be related to the kind of crystal structure. In other words, the thermally stimulated relaxation behaviour of certain luminescent defects appears to be not only dependent on local atomic processes. Triclinic K-feldspars with twinned crystal lattices show an exponential rise and power law decay in the 290 and 440 nm TL bands (Sánchez-Muñoz *et al* 2006b, 2006a). In contrast, symmetric glow curves without power law slope are typical of microstructure-free monoclinic sanidine (Garcia-Guinea *et al* 2003). In this work, new additional data are presented on the thermally stimulated relaxation of x-ray induced defects in a K-feldspar with transitional structure. The crystal analysed here shows a modulated structure at the mesoscopic scale and a unit cell lattice that deviates slightly from monoclinic symmetry. Perhaps the appearance of a glow curve with a small deviation from exponentiality to power law behaviour in the high temperature slope of this crystal is connected with the subtle triclinic distortion in the lattice, i.e. it could be that not only structure but also microstructure plays an essential role in the relaxation dynamics of defects.

Classical models of luminescence are based on band theory, and analyse the phenomenon in simple terms, explaining glow curves only with local electron–hole transitions and short-range atomic order in defect complexes (Randall and Wilkins 1945, Garlick and Gibson 1948). TL curves are supposed to be related to the statistical distribution of trap depth, i.e. energies, below the conduction band. Additionally, that distribution of traps can also be studied with isothermal relaxation experiments. An exponential decay occurs if the local dynamic is governed by electronic transitions between the ground state and the excitation level of the activator, i.e. *the time electrons spend in the recombination centre*. This phenomenon follows exponential behaviour because the underlying electron–hole recombination mechanism is based on a Maxwell–Boltzmann distribution of thermal energy, i.e. lattice vibrations, in which the probability (p) of an electron escaping from the trap at depth E and at temperature T if is governed by (4):

$$p \propto s\, \mathrm{e}^{-E/kT} \tag{4}$$

where s will express the product of the frequency with which the electron strikes the sides of a potential box and the reflection coefficient.

Most triclinic K-rich feldspars are complex mineral systems with a crystal lattice modulated by a long-range elastic field gradient from structures composed of coherent domains at different size scales. This global nature cannot be avoided in explaining the local dynamics during defect induction by irradiation (Sánchez-Muñoz *et al* 2006a), and thus, maybe it must be considered also during the lattice relaxation registered during luminescence emissions. In this system, the isothermal relaxations of radiation-induced defects, monitored by the time evolution of the blue luminescence, follow power law decay laws (Bailiff and Barnett 1994, Wintle 1997, Baril and Huntley 2003, Huntley 2006). The appearance of power law behaviour in both the isothermal and the non-isothermal (TL glow curves) experiments indicates that the time–temperature superposition principle is obeyed (Halpern 1993). This indicates that time and temperature are equivalent variables, i.e. the relaxation mechanism is time and temperature

independent but not the relaxation rate. Thermal lattice vibrations must affect the system behaviour, accelerating the charge recombination process but maintaining the nature of the local processes.

Classical works explain the power law phenomenon by *the time that electrons spend in traps* (Randall and Wilkins 1945) giving rise to continuous trap distributions (CTDs) in non-isothermal experiments, i.e. TL spectra, due to a distribution of activation energies. In addition hyperbolic decays can be explained by the sum of exponential terms (Garlick and Gibson 1948). It is well known that triclinic K-feldspars show CTD (Correcher *et al* 1999). An exponential distribution of traps gives the best fit to the experimental glow peak of a microcline (Sakurai and Gartia 1997). An alternative is to suppose that the glow curve is composed of an infinity of closely disposed single peaks, each with exponential rise and power law decay, due to the underlying continuous nature in the detrapping energy of electrons from their traps. However, it is important to note that while the activation energy increases in the continuous process, the power law slope does not change along the assays. This suggests that the glow curve is not composed of several independent separated peaks. The appearance of two segments in the power law of the studied sample could indicate two different types of crystalline region, for instance from lattices with different triclinicity.

Effect of elastic strain on relaxation

The power law behaviour is typical of the relaxation of complex systems when driven far from equilibrium (Böhmer *et al* 1993, Jonscher *et al* 2003). In particular, four hypotheses have been proposed to explain deviations from exponential decay in luminescence experiments: (i) retrapping in a system composed of a single trapping state and a single recombination centre (Chen and Leung 2003); (ii) tunnelling of trapped electrons to recombinations centres that are randomly distributed (Huntley 2006); (iii) dispersive diffusion (Pavesi and Ceschini 1993); and (iv) many-body interactions (Jonscher and de Polignac 1984). Both the first and second proposals give rise to elegant mathematical descriptions very close to some experimental results, but fail to explain the totality of the available data in this mineralogical system. The tunnelling mechanism is athermal by definition and cannot be used in this case, but could be still applicable in sanidine (Visocekas 2002).

Power law decay of disordered or heterogeneous systems could occur by diffusion of the photoexcited carrier being dispersive because of disorder or heterogeneity in uncorrelated electron–hole pairs (Pavesi and Ceschini 1993), for example hydrogen atomic diffusion in silicon (Kakalios *et al* 1987). In this work, it is proposed that the exponential rise of the glow peak is linked with a luminescence thermally activated by dispersive diffusion of alkali ions, particularly sodium according to previous works (Garcia-Guinea *et al* 1999). If the departure from exponential behaviour is stronger the more relaxing subunits are interconnected with each other, as proposed in Böhmer *et al* (1993), dispersive diffusion solely can explain the profile of glow curves but not the variability between different crystals. Thus, a precise relationship between the atomic cooperativity and certain elements of the microstructure must exist to produce the dispersive behaviour, as well as with the distribution in the activation energies as registered in the CTD.

The hypothesis based on many-body interactions is consistent with the classic assumption that the supply of charge carriers to the recombination centre determines the time dependence. It also suggests that such traps are not acting as independent non-interacting entities in a random system because there is a certain degree of correlation between distant centres (Jonscher and de Polignac 1984). In modern terms, the self-similar luminescence decay could be related to the summation of correlated-cluster systems (Jonscher *et al* 2003) with final power law statistics.

The last two hypotheses can be unified when considering the relationship between the cooperativity, i.e. departure from exponentiality, during the relaxation behaviour and the microstructures linked with the deviation from monoclinic symmetry. Thus, the dispersive character being related to the continuous distribution in the activation energies as registered in the CTD can be linked to a continuous variation of structural strain from the elastic field developed from coherent domain boundaries. Lattice sensitivity to defect formation by irradiation will be maximal at wall boundaries and will decrease with distance, as the spatial distribution of radiation-induced defects from cathodoluminescence images demonstrate (Sánchez-Muñoz *et al* 2006a). Feedback relationships will appear between individual relaxation of radiation-induced defects and the strain distribution along the elastic fields, extended along domains with boundaries as limits of this avalanche effect. Therefore, these long-range correlations between distant defects will produce power law relationships (Burgy *et al* 2004).

The crystalline structural extension in which the collective behaviour is manifested could be correlated with the size of the domains having a coherent relaxation, in other words, by the fractal geometry of the system. In terms of the energy landscape paradigm in crystals, roughness is linked to the microstructure (Van Tendeloo 1997). The modulated structure at the mesoscopic scale involves smooth landscape roughness and then close to exponentiality. The macroscopic twinned lattice can be correlated with macroscopic 'hills' and 'valleys' from coarse domains separated by sharp twin boundaries, and consequently a well developed power law. The non-exponential response is a consequence of the *complexity* of the K-feldspar crystals, with that word meaning additional structure beyond short-range order and the unit cell lattice, i.e. extra periodicity and symmetry because of modulations and twinning. Consequently, the departure from exponential behaviour could be associated with the gradient magnitude of the elastic strain fields inside the domains from twin boundaries (Sánchez-Muñoz *et al* 2006a).

Therefore, the origin of the power law statistic and the complex behaviour at the local level is homologous to that already observed at the macroscopic scale, in K-feldspar, in which the self-organization mechanism is known to occur also with local Si/Al diffusion and collective behaviour of transformation avalanches, as well as in Na-feldspars, with Na/K diffusion in addition to coalescence forming a scale-free size distribution of domains. Accordingly, reciprocity between local self-organizing behaviour and regular patterns formation is induced, that is, local collective-cooperative behaviour can give rise to the formation of regular structures, and vice versa; in a material having that pattern the former behaviour can be stimulated, like happens in the material studied in this paper.

5. Conclusions

This work presents data about the thermally stimulated relaxation of radiation-induced defects, using a TL glow peak at 440 nm, from a transitional K-feldspar in comparison with available information from other K-feldspars. The signal is composed of an exponential rise and a power law decay, indicating that two different processes can be distinguished but that they are intrinsically correlated. The exponential rise indicates that the luminescence process is thermally activated, probably by dispersive diffusion of sodium. The small departure from monoclinic symmetry is correlated with the slight non-exponentiality in the high temperature slope, actually following a power law. The composite shape of the signal has been explained by a feedback relationship between local relaxation of radiation-induced defects and modifications of the global elastic strain field, giving rise to an avalanche effect that could explain the observed power law statistics.

Acknowledgments

We are grateful to Professor Dr P D Townsend for the analyses in the high sensitivity thermoluminescence spectrometer of Sussex (UK), to M L Clarke for recording the 3D-TL measurements, to Mr Olivier Rouer for the EPMA analyses in CNRS (France), and to Ms Leona Nistor and G Van Tendeloo for the TEM and SAED study in EMAT (Belgium). The experimental was supported by the CICYT CGL2004-03564/BTE and Comunidad Autónoma de Madrid MATERNAS (CAM) S-0505/MAT/0094 projects. Thanks are also due to Odulio José Marensi de Moura (Governador Valadares, Minas Geraes, Brasil) for valuable help in the sample collection in the Lavra Fermin.

References

Bailiff I K and Barnett S M 1994 *Radiat. Meas.* **23** 541–5
Bambauer H U, Krause C and Kroll H 1989 *Eur. J. Mineral.* **1** 47–58
Baril M R and Huntley D J 2003 *J. Phys.: Condens. Matter* **15** 8029–48
Böhmer R, Ngai K L, Angell C A and Plazek D J 1993 *J. Chem. Phys.* **99** 4201–9
Bøtter-Jensen L, McKeever S W S and Wintle A G 2003 *Optically Stimulated Luminescence Dosimetry* (Amsterdam: Elsevier)
Burgy J, Moreo A and Dagotto E 2004 *Phys. Rev. Lett.* **92** 097202(4)
Chen R and Leung P L 2003 *Radiat. Meas.* **37** 519–26
Correcher V and Garcia-Guinea J 2001 *J. Lumin.* **93** 303–12
Correcher V, Garcia-Guinea J, Delgado A and Sánchez-Muñoz L 1999 *Radiat. Prot. Dosim.* **84** 503–6
Duller G A T 1997 *Radiat. Meas.* **27** 663–94
Furetta C 2003 *Handbook of Thermoluminescence* (Singapore: World Scientific)
Garcia-Guinea J, Correcher V, Delgado A and Sánchez-Muñoz L 2003 *Radiat. Meas.* **37** 473–7
Garcia-Guinea J, Townsend P D, Sánchez-Muñoz L and Rojo J M 1999 *Phys. Chem. Minerals* **26** 658–67
Garlick G F J and Gibson A F 1948 *Proc. Phys. Soc. London* **60** 574–90
Ghoniem N M, Walgraef D and Zinkle S J 2002 *J. Comput-Aid. Mol. Des.* **8** 1–38
Halpern V 1993 *J. Phys. D: Appl. Phys.* **26** 307–11
Hashimoto T, Nishiyama E and Yanarawa Y 2003 *J. Radioanal. Nucl. Ch.* **255** 81–5
Huntley D J 2006 *J. Phys.: Condens. Matter* **18** 1359–65
Jonscher A K and de Polignac A 1984 *J. Phys. C: Solid State Phys.* **17** 6493–519
Jonscher A K, Jurlewicz A and Veron K 2003 *Contemp. Phys.* **44** 329–39
Kakalios J, Street R A and Jackson W B 1987 *Phys. Rev. Lett.* **59** 1037–40
Kroll H and Ribbe P H 1987 *Am. Mineral.* **72** 491–506
Matyash I V, Bagmut N N, Litovchenko A S and Proshko V Ya 1982 *Phys. Chem. Minerals* **8** 149–52
Pavesi L and Ceschini M 1993 *Phys. Rev.* B **48** 17625–8
Petrov I 1994 *Am. Mineral.* **79** 221–39
Prescott J R and Fox P J 1993 *J. Phys. D: Appl. Phys.* **26** 2245–54
Randall J T and Wilkins M H F 1945 *Proc. R. Soc.* A **184** 390–407
Ribbe P H 1983 *Rev. Mineral* **2** 21–55
Sakurai T and Gartia R K 1997 *J. Appl. Phys.* **82** 5722–7
Sánchez-Muñoz L 1992 Influence of the Na/K exsolutions on the structural and microtextural characteristics of alkali feldspars from pegmatites *PhD Thesis* Universidad Complutense, Madrid, Spain
Sánchez-Muñoz L, Correcher V, Turrero M J, Cremades A and García-Guinea J 2006a *Phys. Chem. Miner.* **33** 639–950
Sánchez-Muñoz L, García-Guinea J, Sanz J, Correcher V and Delgado A 2006b *Chem. Mater.* **18** 3336–42
Sánchez-Muñoz L, Nistor L, Van Tendeloo G and Sanz J 1998 *J. Electron. Microsc.* **47** 17–28
Sánchez-Muñoz L, Rouer O, Sanz J and García-Guinea J 2006c *Bol. Soc. Esp. Ceram.* V **45** 321–9
Smith J V and Brown W L 1988 *Feldspar Minerals* 2nd edn, vol 1 (New York: Springer)
Speit B and Lehmann G 1982 *Phys. Chem. Miner.* **8** 77–82
Van Tendeloo G 1997 *Physica* D **107** 401–6
Visocekas R 2002 *Radiat. Prot. Dos.* **100** 45–54
Wintle A G 1997 *Radiat. Meas.* **27** 769–817